

## Analysis of coined quantum walks with renormalization

Stefan Boettcher and Shanshan Li

Department of Physics, Emory University, Atlanta, Georgia 30322, USA



(Received 8 May 2017; published 12 January 2018)

We introduce a framework to analyze quantum algorithms with the renormalization group (RG). To this end, we present a detailed analysis of the real-space RG for discrete-time quantum walks on fractal networks and show how deep insights into the analytic structure as well as generic results about the long-time behavior can be extracted. The RG flow for such a walk on a dual Sierpinski gasket and a Migdal-Kadanoff hierarchical network is obtained explicitly from elementary algebraic manipulations, after transforming the unitary evolution equation into Laplace space. Unlike for classical random walks, we find that the long-time asymptotics for the quantum walk requires consideration of a *diverging* number of Laplace poles, which we demonstrate exactly for the closed-form solution available for the walk on a one-dimensional loop. In particular, we calculate the probability of the walk to overlap with its starting position, which oscillates with a period that scales as  $N^{d_w^Q/d_f}$  with system size  $N$ . While the largest Jacobian eigenvalue  $\lambda_1$  of the RG flow merely reproduces the fractal dimension,  $d_f = \log_2 \lambda_1$ , the asymptotic analysis shows that the second Jacobian eigenvalue  $\lambda_2$  becomes essential to determine the dimension of the quantum walk via  $d_w^Q = \log_2 \sqrt{\lambda_1 \lambda_2}$ . We trace this fact to delicate cancellations caused by unitarity. We obtain *identical* relations for other networks, although the details of the RG analysis may exhibit surprisingly distinct features. Thus, our conclusions—which trivially reproduce those for regular lattices with translational invariance with  $d_f = d$  and  $d_w^Q = 1$ —appear to be quite general and likely apply to networks beyond those studied here.

DOI: [10.1103/PhysRevA.97.012309](https://doi.org/10.1103/PhysRevA.97.012309)

### I. INTRODUCTION

Quantum walks [1–7] are rapidly achieving a central place in quantum information science. They have captured the imagination because of their wide applicability to describe physical situations as well as computational tasks [6,8–20]. Such a quantum walk, similar to random walks before them [21–24], are completely described by the probability density function (PDF)  $\rho(\vec{x}, t)$  to detect a walk at time  $t$  at a site of distance  $x = |\vec{x}|$  after starting at the origin. At large times and spatial separations, this PDF obeys the scaling collapse,

$$\rho(\vec{x}, t) \sim t^{-\frac{d_f}{d_w}} f(x/t^{\frac{1}{d_w}}), \quad (1)$$

with the scaling variable  $x/t^{1/d_w}$ , where  $d_w$  is the walk dimension and  $d_f$  is the fractal dimension of the network [25].

The evidence that a similar scaling ansatz also describes the behavior of quantum walks on a network is suggested by “weak-limit” results that predict ballistic scaling,  $d_w = 1$ , on  $d$ -dimensional lattices [26,27]. This may be obvious for walks on a lattice in continuous time, which closely resemble the tight-binding model [5,28]. Such a scaling is less obvious for discrete-time quantum walks, which came to prominence as the earliest example for which Grover’s quantum search algorithms [8] can achieve a nearly quadratic speed-up even on a square grid [6,29]. These require an internal “coin” degree of freedom to ensure unitarity, which can impact their spreading behavior in interesting ways, inducing localization without disorder [12,30–32]. It remains largely unexplored how the breaking of translational invariance would affect the asymptotic scaling behavior. That scaling as in Eq. (1) still holds for quantum walks was argued earlier in Ref. [32]. We will show in the following how to *analytically* determine

the spreading dynamics of such a quantum walk on fractal networks. As examples, we explicitly calculate several of the values conjectured there for the walk dimension, in particular, on the dual Sierpinski gasket with  $d_w^Q = \log_2 \sqrt{5}$ , and on a hierarchical network (MK3) with  $d_w^Q = \log_4 \sqrt{21}$ . The existence and nontriviality of those values demonstrate the applicability of Eq. (1). The methods we develop to obtain it allow the study of quantum walks in more complex environments, such as with disorder [33,34] and decoherence [12,35,36].

The renormalization group (RG) of classical random walks [23,25,37] provides a straightforward blueprint for developing the RG for a discrete-time quantum walk, even with the added complication of an internal coin space [38]. In this way, exact RG-flow equations for quantum walks on a number of complex networks have been derived [32,39]. Those results, for instance, have led to the conjecture that the walk dimension  $d_w$  in Eq. (1) for a quantum walk with a Grover coin always is *half* of that for the corresponding random walk,  $d_w^Q = \frac{1}{2} d_w^R$  [39]. Such a relation between classical and quantum scaling has been found previously for the “hitting time” in Markov chains [40,41]. However, the RG analysis of quantum walks is complicated by the unitarity constraint on the evolution operator. As this constraint is not necessarily expressed by the RG recursion equations, we have argued previously [42] that the leading contribution in the RG analysis had to be disregarded to access subdominant terms. Our calculations here demonstrate the subtle and surprisingly diverse ways that unitarity affects the required cancellations in the asymptotic RG analysis. To this end, we explicitly analyze a unitary observable, the amplitude of a quantum walk at its starting position. As this analysis is conducted conveniently via a Laplace transform, a central role is assumed by the Laplace

poles of the observable. While in the RG for classical random walks it is usually sufficient to follow a single pole, for the quantum walk we find it necessary to consider *adiverging* number of such poles to facilitate a consistent evaluation. In light of this, we show how to interpret the fixed point of the RG flow. In particular, we provide an interpretation of eigenvalues of the fixed-point Jacobian. Unlike for the classical case of a random walk [37], the RG flow for a quantum walk must consist of at least two parameters, to yield two relevant eigenvalues. The largest eigenvalue  $\lambda_1$  always reflects merely the geometry of the network under consideration by determining its fractal dimension  $d_f$ , while the dynamics of the quantum walk in the form of its walk dimension  $d_w^Q$  depends on the second eigenvalue  $\lambda_2$ , i.e.,

$$d_f = \log_b \lambda_1, \quad d_w^Q = \log_b \sqrt{\lambda_1 \lambda_2}. \quad (2)$$

These results are obtained for two fractal networks, the dual Sierpinski gasket (DSG) and a Migdal-Kadanoff lattice (MK3) [39,43], where each arrives at the same conclusion in quite distinct fashion, suggesting its generality.

This paper is organized as follows: In Sec. II, we describe the coined quantum walk, its Laplace transform, and its implementation by example of the dual Sierpinski gasket. In Sec. III we derive the generic RG-recursion equations for the DSG. In Sec. IV, we obtain the RG flow for a specific implementation of the quantum walk on a DSG with a Grover coin. In Sec. V, we analyze the fixed point of the RG flow and apply the asymptotic flow to determine the amplitude at the origin of the walk, with some details of the arguments being deferred to the Appendix. In Sec. VI, we compare with the corresponding analysis on a Migdal-Kadanoff lattice. We conclude with a discussion and outlook in Sec. VII.

## II. QUANTUM MASTER EQUATIONS

The time evolution of a discrete-time quantum walk is governed by the evolution equation [6]

$$|\Psi_{t+1}\rangle = \mathcal{U}|\Psi_t\rangle \quad (3)$$

with unitary propagator  $\mathcal{U}$ . With  $\psi_{x,t} = \langle x|\Psi_t\rangle$  in the  $N$ -dimensional site basis  $|x\rangle$  of the network, the probability density function is given by  $\rho(x,t) = |\psi_{x,t}|^2$ . In this basis, the propagator can be represented as a matrix  $\mathcal{U}_{x,y} = \langle x|\mathcal{U}|y\rangle$ , similar to a network Laplacian, but with entries that are operators in an internal coin space which describe the transitions between neighboring sites (“hopping matrices”). We can study the long-time asymptotics via a discrete Laplace transform,

$$\bar{\psi}_x(z) = \sum_{t=0}^{\infty} \psi_{x,t} z^t, \quad (4)$$

as  $z \rightarrow 1^-$  implies the limit  $t \rightarrow \infty$ . So, Eq. (3) becomes

$$\bar{\psi}_x = z \sum_y \mathcal{U}_{x,y} \bar{\psi}_y + \psi_{x,t=0}. \quad (5)$$

Due to the self-similarity of fractal networks, we can decompose  $\mathcal{U}_{x,y}$  into its smallest substructure [37], exemplified by Fig. 1. It shows the elementary graphlet of nine sites that is used to recursively build the DSG of size  $N = 3^g$  after  $g$  generations. The evolution equations in Laplace space

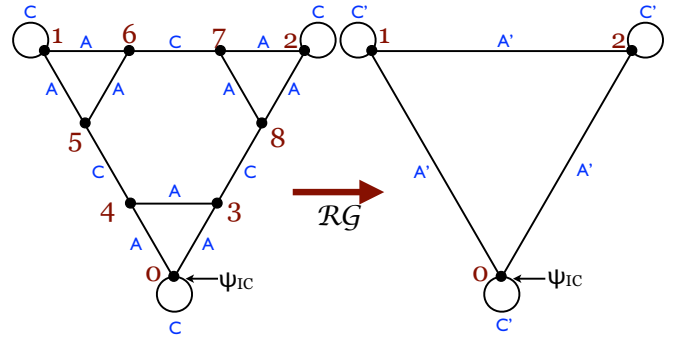


FIG. 1. Depiction of the (final) RG step in the analysis of the DSG. The letters  $\{A, C\}$  label transitions between sites (black dots on the vertices) of the quantum walk in the form of hopping matrices. (Only on the three outermost sites, the matrix  $C$  refers back to the same site.) Recursively, the inner-six sites (labeled 3–8) of each larger triangle (left) in the DSG are decimated to obtain a reduced triangle (right) with renormalized hopping matrices (primed). To build a DSG of  $N = 3^g$  sites, this procedure is applied (in reverse)  $g$  times to all triangles every generation. Each generation the base length  $L$  increases by a factor of  $b = 2$ , such that the fractal dimension is  $d_f = \log_{b=2} 3$ .

pertaining to these sites are

$$\begin{aligned} \bar{\psi}_0 &= (M + C)\bar{\psi}_0 + A(\bar{\psi}_3 + \bar{\psi}_4) + \psi_{IC}, \\ \bar{\psi}_{\{1,2\}} &= (M + C)\bar{\psi}_{\{1,2\}} + A(\bar{\psi}_{\{5,7\}} + \bar{\psi}_{\{6,8\}}), \\ \bar{\psi}_{\{3,4,5,6,7,8\}} &= M\bar{\psi}_{\{3,4,5,6,7,8\}} + C\bar{\psi}_{\{8,5,4,7,6,3\}} \\ &\quad + A(\bar{\psi}_{\{0,3,1,5,2,7\}} + \bar{\psi}_{\{4,0,6,1,8,2\}}). \end{aligned} \quad (6)$$

The hopping matrices  $A$  and  $C$  describe transitions between neighboring sites, while  $M$  permits the walker to remain on its site in a “lazy” walk. The inhomogeneous  $\psi_{IC}$  term allows for an initial condition  $\psi_{x,t=0} = \delta_{x,0}\psi_{IC}$  for a quantum walker to start at site  $x = 0$  in state  $\psi_{IC}$ . (It is tedious but straightforward to generalize the following analysis to an initial condition at arbitrary  $x$  and then treat that entire section of the network accordingly.)

## III. RENORMALIZATION GROUP

We now review the RG procedure for the DSG, as an illustrative example. It is identical to that discussed in Refs. [44,45]. Note that it is a vast improvement over a previous version [32], which assumed that the hopping matrices for each out direction of a site should be distinct. However, the RG recursions (involving five coupled nonlinear recursions with hundreds of terms each in Ref. [32]) significantly simplify here by the assumption of symmetry,  $A = B$ , among the hopping matrices. As a consequence, we obtain a lazy walk to maintain unitarity, as we will discuss in the context of Eq. (13) below.

To accomplish the decimation of the sites  $\bar{\psi}_{\{3,\dots,8\}}$ , as indicated in Fig. 1, we need to solve the linear system in Eqs. (6) for  $\bar{\psi}_{\{0,1,2\}}$ . Thus, we expect that  $\bar{\psi}_{\{3,\dots,8\}}$  can be expressed as (symmetrized) linear combinations:

$$\begin{aligned} \bar{\psi}_{\{3,4\}} &= P\bar{\psi}_0 + Q\bar{\psi}_{\{1,2\}} + R\bar{\psi}_{\{2,1\}}, \\ \bar{\psi}_{\{5,8\}} &= R\bar{\psi}_0 + P\bar{\psi}_{\{1,2\}} + Q\bar{\psi}_{\{2,1\}}, \\ \bar{\psi}_{\{6,7\}} &= Q\bar{\psi}_0 + P\bar{\psi}_{\{1,2\}} + R\bar{\psi}_{\{2,1\}}. \end{aligned} \quad (7)$$

Inserting this ansatz into Eqs. (6) and comparing coefficients provides consistently for the unknown matrices:

$$\begin{aligned} P &= (M + A)P + A + CR, \\ Q &= (M + C)Q + AR, \\ R &= MR + AQ + CP. \end{aligned} \quad (8)$$

Using the abbreviations  $S = (\mathbb{I} - M - C)^{-1}A$  and  $T = (\mathbb{I} - M - AS)^{-1}C$ , Eqs. (8) have the solution

$$\begin{aligned} P &= (\mathbb{I} - M - A - CT)^{-1}A, \\ R &= TP, \\ Q &= SR. \end{aligned} \quad (9)$$

Finally, after  $\bar{\psi}_{\{3,\dots,8\}}$  have been eliminated, we find

$$\bar{\psi}_0 = ([M + 2AP] + C)\bar{\psi}_0 + A(Q + R)(\bar{\psi}_1 + \bar{\psi}_2) + \psi_{IC}, \quad (10)$$

and similar for  $\bar{\psi}_{\{1,2\}}$  (without  $\psi_{IC}$ ). By comparing coefficients between the renormalized expression in Eq. (10) and the corresponding *self-similar* expression in the first line of Eqs. (6), we can identify the RG recursions

$$\begin{aligned} M_{k+1} &= M_k + 2A_k P_k, \\ A_{k+1} &= A_k(Q_k + R_k), \\ C_{k+1} &= C_k, \end{aligned} \quad (11)$$

where the subscripts refer to  $k$ - and  $(k + 1)$ -renormalized forms of the hopping matrices. These recursions evolve from the unrenormalized ( $k = 0$ ) hopping matrices with

$$\{M, A, C\}_{k=0} = z\{M, A, C\}. \quad (12)$$

These RG recursions are entirely generic and, in fact, would hold for any walk on the DSG, classical or quantum. In the following, we now consider a specific form of a quantum walk with a Grover coin.

#### IV. RG FLOW FOR THE QUANTUM WALK WITH A GROVER COIN

To study the scaling solution for the spreading quantum walk according to Eq. (1), it is sufficient to investigate the properties of the RG recursion in Sec. III for  $\{M, A, C\}$ . In the unrenormalized (“raw”) description of the walk, these hopping matrices are chosen as

$$\begin{aligned} M &= \begin{bmatrix} -\frac{1}{3} & 0 & 0 \\ 0 & 1 & 0 \\ 0 & 0 & 0 \end{bmatrix} G, \\ A &= \begin{bmatrix} \frac{2}{3} & 0 & 0 \\ 0 & 0 & 0 \\ 0 & 0 & 0 \end{bmatrix} G, \quad C = \begin{bmatrix} 0 & 0 & 0 \\ 0 & 0 & 0 \\ 0 & 0 & 1 \end{bmatrix} G. \end{aligned} \quad (13)$$

Here, we have to pay a small price for the fact that, throughout,  $A$  shifts weights *symmetrically* to two neighboring sites within their local triangle. The walk now must have a lazy component, i.e., some weight may remain at each site every update, so that  $M \neq 0$ . Only then does the walk satisfy the unitarity conditions derived for the DSG in Ref. [44]. The matrix  $C$  shifts weight to the one neighbor outside those triangles, as illustrated in Fig. 1.

These weights are the three complex components of the state vector at each site,  $\psi_{x,t}$ , which are all zero at  $t = 0$ , except at  $x = 0$  where  $\psi_{x=0,t=0} = \psi_{IC}$  is arbitrary but normalized,  $|\psi_{IC}^2| = 1$ . For every update, these weights are entangled at each site before every shift via the unitary  $3 \times 3$  coin matrix due to Grover, which is given by

$$G = \frac{1}{3} \begin{bmatrix} -1 & 2 & 2 \\ 2 & -1 & 2 \\ 2 & 2 & -1 \end{bmatrix}. \quad (14)$$

The walk is unitary, i.e., the norm stays preserved, because  $G$  is unitary and  $2A + C + M = \mathbb{I}$ . Note that  $G$  is also reflective, i.e.,  $G^2 = \mathbb{I}$ .

Iterating the RG recursions in Sec. III for the matrices in Eq. (13) for only the  $k = 1$  step reveals a simple recursive pattern that suggests the ansatz

$$\begin{aligned} M_k &= \begin{bmatrix} \frac{a_k}{3} - \frac{2b_k}{3} & 0 & 0 \\ 0 & z & 0 \\ 0 & 0 & 0 \end{bmatrix} G, \\ A_k &= \begin{bmatrix} \frac{a_k}{3} + \frac{b_k}{3} & 0 & 0 \\ 0 & 0 & 0 \\ 0 & 0 & 0 \end{bmatrix} G, \quad C_k = \begin{bmatrix} 0 & 0 & 0 \\ 0 & 0 & 0 \\ 0 & 0 & z \end{bmatrix} G. \end{aligned} \quad (15)$$

This flow is initiated already at  $k = 0$  with

$$a_{k=0} = b_{k=0} = z. \quad (16)$$

Inserted into the RG recursions in Sec. III, these matrices exactly reproduce themselves *in form* after one iteration,  $k \rightarrow k + 1$ , when we identify for the scalar RG flow

$$\begin{aligned} a_{k+1} &= \frac{3(3z - 1)a_k b_k + (3 - z)(a_k - 2b_k)}{3(3 - z) - (3z - 1)(2a_k - b_k)}, \\ b_{k+1} &= \frac{3(3z - 1)(3z^2 + 1)a_k b_k^2 + 2(3z^3 - 3z^2 + 7z - 3)b_k^2 - 4(3z^3 - 6z^2 + 4z - 3)a_k b_k - (3 - z)(3 + z^2)(a_k - 2b_k)}{(3z - 1)(3z^2 + 1)(2a_k - b_k)b_k - 2(3z^3 - 7z^2 + 3z - 3)a_k + 4(3z^3 - 4z^2 + 6z - 3)b_k + 3(3 - z)(3 + z^2)}. \end{aligned} \quad (17)$$

Note that these RG-flow recursions are vastly simpler than the five-term recursions previously reported [32].

#### V. RG ANALYSIS FOR THE DSG

We now proceed to study the fixed-point properties of the RG flow at  $k \sim k + 1 \rightarrow \infty$  near  $z \rightarrow 1$ , which builds on the discussion in Ref. [42]. With the choice of  $a_k$  and  $b_k$  in Eq. (15), the Jacobian matrix  $J = \frac{\partial(a_{k+1}, b_{k+1})}{\partial(a_k, b_k)} \Big|_{k \rightarrow \infty}$  of the fixed point at  $z = 1$  and  $a_\infty = b_\infty = 1$  already is diagonal, with two eigenvalues,  $\lambda_1 = 3$  and  $\lambda_2 = \frac{5}{3}$ . The eigenvalues correspond to those two of the five eigenvalues found in Ref. [32] that are relevant, i.e., they are  $> 1$ . Extending the expansion of Eq. (17) in powers of  $\zeta = z - 1$  for  $k \rightarrow \infty$  to higher order, we obtain

$$\begin{aligned} a_k(z) &\sim 1 + \zeta^1 \mathcal{A} \lambda_1^k + \zeta^2 \alpha_k^{(2)} + \zeta^3 \alpha_k^{(3)} + \dots, \\ b_k(z) &\sim 1 + \zeta^1 \mathcal{B} \lambda_2^k + \dots, \end{aligned} \quad (18)$$

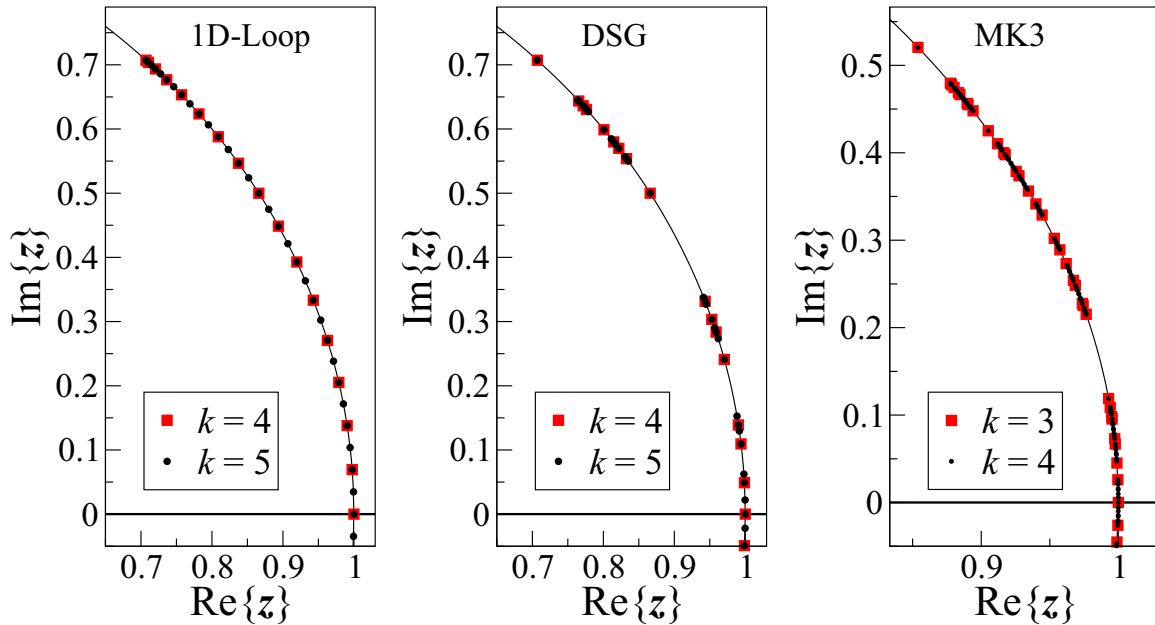


FIG. 2. Plot of the poles of the Laplace transforms for the amplitude to remain at the origin,  $\bar{\psi}_0^{(k)}(z) = X_k \psi_{IC}$ , in the complex- $z$  plane at two consecutive RG steps  $k$  for a quantum walk on the 1D line (left), DSG (middle), and MK3 (right). (In these walks, poles are certain to occur in complex-conjugate pairs, so only the upper  $z$  plane is shown.) Although the pattern by which poles evolve appears more complicated for the DSG and MK3, a diverging number of those poles progressively impinge on the real- $z$  axis for all systems.

with unknown constants  $\mathcal{A}$  and  $\mathcal{B}$ , and with

$$\begin{aligned} \alpha_k^{(2)} &\sim \frac{1}{2}(\mathcal{A}\lambda_1^k)^2 + \dots, \\ \alpha_k^{(3)} &\sim \frac{1}{4}(\mathcal{A}\lambda_1^k)^3 - \frac{1}{8}(\mathcal{A}\lambda_1^k)^2(\mathcal{B}\lambda_2^k) + \dots, \end{aligned} \quad (19)$$

where we have only kept leading-order terms in  $k$  that contribute in the following considerations.

For the case of a classical random walk, only the dominant eigenvalue  $\lambda_1$  would be relevant to determine  $d_w^R = \log_2 \lambda_1$  [37]. In contrast, in Ref. [42] it was conjectured that for a quantum walk the Jacobian eigenvalues provide  $d_f$  and  $d_w^Q$  as given in Eq. (2). Here, we shall scrutinize that claim in more detail and show explicitly how to calculate both exponents. Central to this argument is the fact that the observable  $\rho(x, t) = |\psi_{x,t}^2|$  in Eq. (1) has Laplace poles that only move with  $k$  on the unit circle in the complex  $z$  plane, while those poles of  $a_k$  and  $b_k$  move both tangentially and radially on the outside of that circle. That radial motion with  $k$ —absent in  $\bar{\rho}(x, z)$ —depends only on  $\lambda_1$ , while the tangential motion is controlled by  $\sqrt{\lambda_1 \lambda_2}$ . This conclusion was based on modeling the behavior of just the two complex poles closest to  $z = 1$ . Although these conclusions turn out to be correct, a more detailed analysis shows that actually  $o(N)$  of such poles impinging on  $z = 1$  must be considered here, which is significant. This we can demonstrate rigorously in the Appendix for the case of a quantum walk on the one-dimensional (1D) line. Here, we will utilize the implications of that discussion for our analysis of the DSG.

Instead of  $\bar{\rho}(x, z)$  in its entirety, we focus merely on  $\bar{\psi}_0(z)$ , the amplitude at the origin of the quantum walk on the DSG.

According to Fig. 1 and Eq. (10), we have

$$\begin{aligned} \bar{\psi}_0 &= (M_k + C_k)\bar{\psi}_0 + A_k(\bar{\psi}_1 + \bar{\psi}_2) + \psi_{IC}, \\ \bar{\psi}_{\{1,2\}} &= (M_k + C_k)\bar{\psi}_{\{1,2\}} + A_k(\bar{\psi}_0 + \bar{\psi}_{\{2,1\}}), \end{aligned} \quad (20)$$

which has the solution  $\bar{\psi}_0 = X_k \psi_{IC}$  with

$$X_k = [\mathbb{I} - M_k - C_k - 2A_k(\mathbb{I} - M_k - A_k - C_k)^{-1}A_k]^{-1}. \quad (21)$$

Inserting Eqs. (15) and (18) and expanding (some generic component of) the matrix  $X_k$  in powers of  $\zeta = z - 1$  yields

$$\begin{aligned} [X_k]_{11} &\sim -\zeta^{-1} \frac{1}{9(\mathcal{A}\lambda_1^k)} + \zeta^0 \left[ \frac{4}{9} + \frac{\alpha_k^{(2)}}{9(\mathcal{A}\lambda_1^k)^2} \right] \\ &\quad + \zeta^1 \left[ \frac{(\mathcal{A}\lambda_1^k)\alpha_k^{(3)} - (\alpha_k^{(2)})^2}{9(\mathcal{A}\lambda_1^k)^3} + \frac{1}{3}(\mathcal{B}\lambda_2^k) \right] + \dots \\ &\sim \zeta^{-1} O\left(\frac{1}{\lambda_1^k}\right) + \zeta^0 O(1) + \zeta^1 O(\lambda_2^k) + \dots \end{aligned} \quad (22)$$

It is the cancellation of the leading  $O(\lambda_1^k)$  term at order  $\zeta^{-1}$  that signals the anticipated placement of the Laplace poles onto the unit circle in the complex  $z$  plane, as demanded by unitarity. As argued in Ref. [42],  $\lambda_1$  controls the radial movement of poles with  $k$  which is removed by this cancellation, thereby exposing  $\lambda_2^k$  as the relevant contribution that controls the tangential movement of poles purely on the unit circle. Numerical studies of the Laplace poles of  $X_k$  for small values of  $k$ , shown in Fig. 2, suggest that these poles arise along arcs on the unit circle, located symmetrically around the real- $z$  axis due to the real-valued coin such as  $G$  in Eq. (14), and that these poles get increasingly dense and impinge on the real- $z$  axis at  $z = 1$ .

This picture is borne out by our analysis of a quantum walk on the 1D loop in the Appendix, which suggests the following generalized form for the amplitude matrix at the origin:

$$\begin{aligned}
 [X_k]_{11} &\sim \frac{1}{h(N)} \sum_{j=-h(N)}^{h(N)} \frac{f_j}{1 - z e^{i\theta_k j g_j}} \\
 &\sim -\zeta^{-1} \frac{f_0}{h(N)} + \zeta^0 \frac{2S_0(N)}{h(N)} - \zeta^1 \frac{4S_2(N)}{\theta_k^2 h(N)} + \dots,
 \end{aligned} \tag{23}$$

where we defined the sums

$$S_m(N) = \sum_{j=1}^{h(N)} \frac{f_j}{(g_j j)^m}. \tag{24}$$

By analogy with the 1D loop, we expect by the fact that the coin in Eq. (14) is reflective and real that both  $f_j$  and  $g_j$  are real, symmetric, and weakly varying functions of  $j$  (but not  $N$ ). In turn,  $h(N)$  specifies how many Laplace poles effectively contribute to the asymptotic behavior. If only one (or few) poles contribute,  $h(N) = O(1)$ , as in the classical case [37], then  $S_m = O(1)$  for all  $m \geq 0$ , and the  $\zeta^0$  terms between Eqs. (22) and (23) are inconsistent. The only consistent choice entails that a diverging number of poles must be considered,  $h(N) \gg 1$ , specifically  $h(N) \sim \lambda_1^k = N$ . This implies that (a)  $S_0 = O(N)$  and (b)  $S_{m \geq 2} = O(1)$ . For instance, in the 1D quantum walk, we have  $f_j = g_j = \text{const}$  such that both (a) and (b) are satisfied. Matching the expansion also between the  $\zeta^1$  terms of Eqs. (22) and (23), we obtain  $\theta_k^2 h(N) \sim \lambda_2^{-k}$  or  $\theta_k^2 \sim \lambda_1^{-k} \lambda_2^{-k}$ . With  $L = 2^k$  and assuming that the scaling solution implied by Eq. (1) arises via the cutoff at  $\theta_k t \sim 1$  [37], i.e.,  $\theta_k \sim L^{-d_w^0}$ , we arrive at Eq. (2). Expanding to two more orders in powers of  $\zeta$  provides further proof of the consistency of this interpretation.

The backwards Laplace transform of  $X_k$  in Eq. (23) provides for some typical component in the spinor  $\psi_{0,t}$  in a DSG of size  $N = 3^k$  that

$$\psi_{0,t} \sim \frac{1}{h(N)} \sum_{j=0}^{h(N)} f_j \cos\left(\frac{j g_j t}{N^{d_w^0/d_f}}\right). \tag{25}$$

Note that due to condition (a) we have  $|\psi_{0,t}^{(k)}| \sim 1$  for  $t = 0$ , as would be expected for a walk starting at  $x = 0$ .

## VI. RG ANALYSIS FOR MK3

To demonstrate the generality of our conclusions, we present briefly also the corresponding analysis for another fractal network, based on the Migdal-Kadanoff hierarchical lattices [43,46]. The RG recursions, as depicted in Fig. 3, for this case have already been presented in detail previously in Ref. [39]. Again, all matrices can be parametrized with merely two scalars, most conveniently in the form  $\{A, B, C\} = \frac{a+b}{2}(P_{\{1,2,3\}} \cdot G)$  and  $M = \frac{a-b}{2}(\mathbb{I} \cdot G)$ , where the  $3 \times 3$  matrices  $[P_v]_{i,j} = \delta_{i,v} \delta_{v,j}$  (with  $\sum_{v=1}^3 P_v = \mathbb{I}$ ) facilitate the shift of the  $v$ th component to a neighboring site. The RG flow was found

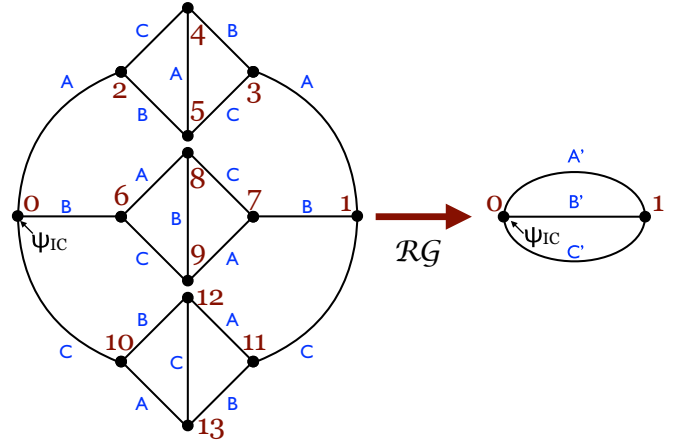


FIG. 3. Graphic depiction of the (final) RG step in the analysis of MK3. The letters  $\{A, B, C\}$  label transitions between sites (black dots on the vertices) of the quantum walk in the form of hopping matrices. Recursively, the inner-four sites (here labeled 2–5, 6–9, and 10–13) of each branch in MK3 are decimated to obtain a reduced set of three lines (right) with renormalized hopping matrices (primed). To build MK3 of  $N = 2 \times 7^g$  sites, this procedure is applied in reverse  $g$  times to all lines at each generation. Note that each generation the base length  $L$  increases by a factor of 4, such that the fractal dimension is  $d_f = \log_4 7$ .

to close for

$$\begin{aligned}
 a_{k+1} &= \frac{-9a_k + 5a_k^3 + 9b_k + 3a_k b_k - 17a_k^2 b_k - 3a_k^3 b_k + 3b_k^2 + 14a_k b_k^2 - 3a_k^2 b_k^2 - 18a_k^3 b_k^2}{-18 - 3a_k + 14a_k^2 + 3a_k^3 - 3b_k - 17a_k b_k + 3a_k^2 b_k + 9a_k^3 b_k + 5b_k^2 - 9a_k^2 b_k^2}, \\
 b_{k+1} &= \frac{-3a_k - a_k^2 + 3b_k + 4a_k b_k - 3a_k^2 b_k - b_k^2 + 3a_k b_k^2 + 6a_k^2 b_k^2}{6 + 3a_k - a_k^2 - 3b_k + 4a_k b_k + 3a_k^2 b_k - b_k^2 - 3a_k b_k^2},
 \end{aligned} \tag{26}$$

with  $a_0 = b_0 = z$ . Remarkably, it can be shown that  $|a_k| = |b_k| \equiv 1$  for all  $k$ , in principle reducing the RG parameters to just two real phases for  $a_k, b_k$ .

Similar to the DSG in Sec. V, we have a fixed point at  $z = 1$  with  $a_\infty = b_\infty = 1$ . Again, the Jacobian already is diagonal with the two eigenvalues,  $\lambda_1 = 7$  and  $\lambda_2 = 3$ . As before, extending the expansion of Eq. (17) in powers of  $\zeta = z - 1$  for  $k \rightarrow \infty$  to higher order, we obtain

$$\begin{aligned}
 a_k(z) &\sim 1 + \zeta \mathcal{A} \lambda_1^k + \zeta^2 \alpha_k^{(2)} + \zeta^3 \alpha_k^{(3)} + \dots, \\
 b_k(z) &\sim 1 + \zeta \mathcal{B} \lambda_2^k + \zeta^2 \beta_k^{(2)} + \zeta^3 \beta_k^{(3)} + \dots,
 \end{aligned} \tag{27}$$

with unknown constants  $\mathcal{A}$  and  $\mathcal{B}$ , and with

$$\begin{aligned}
 \alpha_k^{(2)} &\sim \frac{1}{2} (\mathcal{A} \lambda_1^k)^2 + \dots, \\
 \alpha_k^{(3)} &\sim \frac{1}{4} (\mathcal{A} \lambda_1^k)^3 + \dots, \\
 \beta_k^{(2)} &\sim \frac{1}{2} (\mathcal{B} \lambda_2^k)^2 + \dots, \\
 \beta_k^{(3)} &\sim -\frac{3}{80} (\mathcal{A} \lambda_1^k) (\mathcal{B} \lambda_2^k)^2 + \dots,
 \end{aligned} \tag{28}$$

where we have only kept leading-order terms in  $k$  relevant for the following considerations.

The final step of the RG, shown on the right of Fig. 3, is given by

$$\begin{aligned}\bar{\psi}_0 &= M_k \bar{\psi}_0 + (A_k + B_k + C_k) \bar{\psi}_1 + \psi_{IC}, \\ \bar{\psi}_1 &= M_k \bar{\psi}_1 + (A_k + B_k + C_k) \bar{\psi}_0,\end{aligned}\quad (29)$$

which has the solution  $\bar{\psi}_0 = X_k \psi_{IC}$  with

$$X_k = [\mathbb{I} - M_k - V_k(\mathbb{I} - M_k)^{-1} V_k]^{-1}, \quad (30)$$

abbreviating  $V_k = A_k + B_k + C_k$ . Inserting  $\{A_k, B_k, C_k, M_k\}$  with the RG flow in Eq. (27) into  $X_k$  in Eq. (30) and expanding in powers of  $\zeta = z - 1$  yields for the (1, 1) component

$$\begin{aligned}[X_k]_{11} &\sim -\zeta^{-1} \left[ \frac{1}{3(\mathcal{B}\lambda_2^k)} + \frac{1}{6(\mathcal{A}\lambda_1^k)} \right] + \zeta^0 \left[ \frac{1}{4} + \dots \right] \\ &+ \zeta^1 \left[ \frac{(\mathcal{A}\lambda_1^k)\alpha_k^{(3)} - (\alpha_k^{(2)})^2}{6(\mathcal{A}\lambda_1^k)^3} - \frac{23(\mathcal{A}\lambda_1^k)}{240} + \dots \right] \\ &+ \dots \\ &\sim \zeta^{-1} \mathcal{O}\left(\frac{1}{\lambda_2^k}\right) + \zeta^0 \mathcal{O}(1) + \zeta^1 \mathcal{O}(\lambda_1^k) + \dots\end{aligned}\quad (31)$$

Although the  $\zeta^1$  term exhibits the same cancellation in the first term as in Eq. (22) for the DSG, other terms of order  $\mathcal{O}(\lambda_1^k)$  remain, hiding any contributions from  $\lambda_2$  here. However, the highly peculiar  $\zeta^{-1}$  term *also* reverses the role of the eigenvalues, now selecting  $\lambda_2$  as the dominant contribution over  $\lambda_1$  there. Comparison with the expected form of  $X_k$  in Eq. (23) then leads to an effective number of poles that scales subextensively with the system size,  $h(N) \sim \lambda_2^k = N^{\log_5 3}$ . Consistency then also demands that  $S_0(N) \sim h(N)$ , so that  $S_{m \geq 2}(N) = \mathcal{O}(1)$ . Amazingly, despite the reversal of roles between  $\lambda_1$  and  $\lambda_2$ , matching the  $\zeta^1$  terms again provides  $\theta_k^2 \sim \lambda_1^{-k} \lambda_2^{-k}$ , which is invariant to this switch. As before, we have expanded to two more orders in powers of  $\zeta$  and found consistency throughout. Thus, the RG of MK3 affirms the result in Eq. (2), all differences in the analysis aside.

## VII. DISCUSSION

We have provided a comprehensive description of the real-space renormalization-group treatment of discrete-time quantum walks. We have referred to the DSG and MK3 as specific examples, but we expect that this procedure also describes other networks. Our procedure is immediately applicable to study the quantum search algorithm with a coin or power-law localization in hierarchical networks, which we will present elsewhere. Especially, our approach opens the door to a systematic consideration of universality classes in quantum walks and search algorithms. For instance, entire classes of coins can be studied, in particular those that might break the symmetries that were essential to establish the current results and the delicate cancellations these require. The methods developed here also provide the starting point for the consideration of disordered environments [33,34] and the discussion of localization in complex networks [32]. Finally, approximate means can be explored on the basis of the current calculation that eventually can preserve unitarity, or allow one to handle decoherence in a controlled manner that is found in any realistic implementations [10,12,35].

## ACKNOWLEDGMENTS

S.B. acknowledges financial support from Conselho Nacional de Desenvolvimento Científico e Tecnológico (CNPq) in Brazil through the ‘‘Ciência sem Fronteiras’’ program and thanks Laboratório Nacional de Computação Científica (LNCC) in Petropolis, Brazil for its hospitality. S.L. is supported by the Program to Enhance Research and Scholarship (PERS) at Emory University.

## APPENDIX: ANALYSIS OF THE QUANTUM WALK ON A LINE

The renormalization group treatment of the quantum walk on the 1D line [38] provides the RG flow:

$$\begin{aligned}a_{k+1} &= \frac{\sin \eta a_k^2}{1 - 2 \cos \eta b_k + b_k^2}, \\ b_{k+1} &= b_k + \frac{(b_k - \cos \eta) a_k^2}{1 - 2 \cos \eta b_k + b_k^2}.\end{aligned}\quad (A1)$$

But unlike the analog expressions for the DSG in Eq. (17) or MK3 in Eq. (26), this RG flow in fact possesses a closed-form solution for all  $N = 2^k$ :

$$a_k = \frac{\cos \sigma \sin \eta}{\cos(N\nu + \sigma)}, \quad b_k = \cos \eta + i \frac{\sin(N\nu) \sin \eta}{\cos(N\nu + \sigma)}, \quad (A2)$$

where  $\nu(z)$  and  $\sigma(z)$  are determined by matching to the initial flow,  $a_1 = z^2 \sin \eta$  and  $b_1 = z^2 \cos \eta$ .

Previously, in Ref. [42], the equivalent of Eq. (21) for the amplitude at the starting site of a quantum walk,  $\psi_0 = X_k \psi_{IC}$ , for the 1D line was shown to be

$$X_k = [\mathbb{I} - (A_k + B_k + M_k)]^{-1}. \quad (A3)$$

Here, the hopping matrices are parametrized as

$$A_k = \begin{bmatrix} a_k & 0 \\ 0 & 0 \end{bmatrix} \mathcal{C}, \quad B_k = \begin{bmatrix} 0 & 0 \\ 0 & -a_k \end{bmatrix} \mathcal{C}, \quad M_k = \begin{bmatrix} 0 & b_k \\ b_k & 0 \end{bmatrix} \mathcal{C} \quad (A4)$$

after  $k$  renormalization steps, with the coin matrix

$$\mathcal{C} = \begin{pmatrix} \sin \eta & \cos \eta \\ \cos \eta & -\sin \eta \end{pmatrix}. \quad (A5)$$

Equations (A2)–(A4) together provide

$$\begin{aligned}X_k &= \frac{\begin{bmatrix} 1 - a_k \sin \eta - b_k \cos \eta & a_k \cos \eta - b_k \sin \eta \\ -a_k \cos \eta + b_k \sin \eta & 1 - a_k \sin \eta - b_k \cos \eta \end{bmatrix}}{1 - 2a_k \sin \eta - 2b_k \cos \eta + a_k^2 + b_k^2} \\ &= \begin{bmatrix} \frac{1}{2} & -\frac{\cot \eta}{2} \\ \frac{\cot \eta}{2} & \frac{1}{2} \end{bmatrix} + \frac{\begin{bmatrix} i \cot \eta + \sin \sigma & i - \sin \sigma \cot \eta \\ \sin \sigma \cot \eta - i & i \cot \eta + \sin \sigma \end{bmatrix}}{2 \tan \frac{N\nu}{2} \cos \sigma}.\end{aligned}\quad (A6)$$

In the following, we shall express  $X_k$  asymptotically near the RG fixed point for  $\zeta = z - 1 \rightarrow 0$  and  $N = 2^k \rightarrow \infty$  in *three* different ways: (1) the exact solution, (2) the presumed expansion in  $\mathcal{O}(N)$  Laplace poles, and (3) the expansion of the RG flow in Eq. (A1), which is typically the only form available in nontrivial applications of the RG. The validation of 2 and

3 by 1 demonstrates our contention that, indeed, a number of Laplace poles must be considered that diverges with  $N$  to consistently interpret 3.

**1. Exact solution**

We simplify matters and (without restriction of generality) set  $\eta = \frac{\pi}{4}$  in the following. With  $a_1 = b_1 = z^2/\sqrt{2}$  we find from Eq. (A2) that

$$\begin{aligned} \sin 2\nu &= i \left( \frac{1}{z^2} - 1 \right) \sqrt{1+z^4}, \\ \sin \sigma &= i z^2. \end{aligned} \tag{A7}$$

The expansion of Eq. (A2) in powers of  $\zeta = z - 1$  is now straightforward and results in

$$\begin{aligned} a_k &\sim \zeta^0 \frac{1}{\sqrt{2}} + \zeta^1 \frac{N}{\sqrt{2}} + \zeta^2 \frac{N}{2\sqrt{2}} \\ &\quad - \zeta^3 \frac{2(N-2)(N-1)N}{3\sqrt{2}} \\ &\quad - \zeta^4 \frac{(N-2)N(3N^2-8N+2)}{6\sqrt{2}} \dots, \\ b_k &\sim \zeta^0 \frac{1}{\sqrt{2}} + \zeta^1 \frac{N}{\sqrt{2}} + \zeta^2 \frac{N(2N-3)}{2\sqrt{2}} \\ &\quad + \zeta^3 \frac{(N-2)(N-1)N}{3\sqrt{2}} \\ &\quad - \zeta^4 \frac{(N-2)N(4N^2-6N+5)}{12\sqrt{2}} + \dots \end{aligned} \tag{A8}$$

Inserted into Eq. (A6), we find for each component of the matrix  $X_k$  in Eq. (A6)

$$\begin{aligned} [X_k]_{11} &= [X_k]_{22} \sim -\zeta^{-1} \frac{1}{N} + \zeta^0 \frac{N-1}{2N} - \zeta^1 \frac{2N^2-5}{12N} + \dots, \\ [X_k]_{12} &= -[X_k]_{21} \sim \zeta^{-1} 0 - \zeta^0 \frac{N-2}{2N} + \zeta^1 0 + \dots \end{aligned} \tag{A9}$$

Note that a larger number of terms in Eq. (A8) is needed that could potentially contribute to second order in Eq. (A9), due to the singular nature of  $X_k$ . However, to leading order in  $N$  in  $X_k$ , those terms finally do cancel.

**2. Expansion in Laplace poles**

The long-range asymptotics (in space and time) of  $X_k$  is determined by its Laplace poles in the complex  $z$  plane [42]. As shown in Fig. 2, unitarity demands that these poles are all located on the unit circle there, and we can parametrize them as  $z_j = e^{i\omega_j}$ . With  $a_1 = b_1 = z^2/\sqrt{2}$  we find from Eq. (A7) on the unit circle

$$\sin \nu_j = -\sqrt{2} \sin \omega_j, \quad \sin \sigma_j = i e^{2i\omega_j}. \tag{A10}$$

To find the Laplace poles of  $X_k$  in the second line of Eq. (A6), we can ignore the first (nonsingular) matrix and focus on the  $N$ -dependent zeros of the denominator of the second,

$$\nu_j = \frac{2\pi}{N} j \sim -\sqrt{2}\omega_j, \quad (j \in \mathbb{Z}), \tag{A11}$$

in accordance with Fig. 2. Note, again, that such a result,  $\omega_j = j\theta_k$  with

$$\theta_k = \frac{\sqrt{2}\pi}{N}, \tag{A12}$$

can only be obtained because we are in possession of the closed-form solution of the RG flow. It will be the purpose of the next section, and of the entire RG analysis generally, to produce the scaling of the cutoff in time,  $1/\theta_k$ , with system size  $N$ .

At small  $\omega_j$ , we also have from Eq. (A10) that  $\sin \sigma_j \sim i - 2\omega_j$  and  $\cos \sigma_j \sim \sqrt{2}$ . To evaluate the residue of  $X_k$  at the  $j$ th pole, we obtain

$$R_j = \lim_{z \rightarrow e^{i\omega_j}} (z - e^{i\omega_j}) X_k \sim -\frac{1}{N} \begin{bmatrix} 1 & -i\omega_j \\ i\omega_j & 1 \end{bmatrix} \sim -\frac{1}{N} \mathbb{I}, \tag{A13}$$

to leading order. Using  $\omega_j = j\theta_k$ , we then express (some component of)  $X_k$  in terms of  $h(N) = O(N)$  of such poles:

$$\begin{aligned} X_k &\sim \sum_{j=-h(N)}^{h(N)} \frac{R_j}{z - e^{i\theta_k j}}, \\ [X_k]_{11} &\sim -\zeta^{-1} \frac{1}{N} - \frac{1}{N} \sum_{j=1}^{h(N)} \left[ \frac{1}{\zeta+1-e^{i\theta_k j}} + \frac{1}{\zeta+1-e^{-i\theta_k j}} \right] \\ &\sim -\zeta^{-1} \frac{1}{N} - \frac{1}{N} \sum_{j=1}^{h(N)} \left[ \zeta^0 + \zeta^1 \frac{2}{\theta_k^2 j^2} + \dots \right] \\ &\sim -\zeta^{-1} \frac{1}{N} - \zeta^0 \frac{h(N)}{N} - \zeta^1 \left( \sum_{j=1}^{h(N)} \frac{1}{j^2} \right) \frac{2}{N\theta_k^2} + \dots \end{aligned} \tag{A14}$$

The last line must be compared with the exact result in Eq. (A9). The first term fits exactly, and the last term does fit with the correct choice of  $\theta_k$  in Eq. (A12) and the realization that the sum is always finite, whether  $h(N)$  is small or divergent. The key observation concerns the middle term: There, the comparison demands that  $h(N) \sim N$ , i.e., that we must sum over  $O(N)$  poles to make the match consistent. We thus conjecture this to be generically true. In fact, the application of this conjecture allows us to consistently interpret the results for the DSG (and other networks).

**3. RG-flow solution**

Typically, such as for the case of the DSG in Eq. (17) or MK3 in Eq. (26), we do not possess a closed-form solution of the RG flow like Eq. (A2). In those cases, we would proceed as in Sec. IV to obtain the asymptotic expansion of the RG flow by expanding around the fixed point at  $z = 1$ . This expansion [38] finds the Jacobian eigenvalues  $\lambda_1 = \lambda_2 = 2$  to first order and continues to yield

$$\begin{aligned} a_k(z) &\sim \frac{1}{\sqrt{2}} + \zeta \mathcal{A} \lambda_1^k + \zeta^2 \alpha_k^{(2)} + \zeta^3 \alpha_k^{(3)} + \dots, \\ b_k(z) &\sim \frac{1}{\sqrt{2}} + \zeta \mathcal{B} \lambda_2^k + \zeta^2 \beta_k^{(2)} + \zeta^3 \beta_k^{(3)} + \dots, \end{aligned} \tag{A15}$$

with

$$\begin{aligned}\alpha_k^{(2)} &\sim \frac{1}{\sqrt{2}}(\mathcal{A}\lambda_1^k)^2 - \frac{1}{\sqrt{2}}(\mathcal{B}\lambda_2^k)^2 + \dots, \\ \alpha_k^{(3)} &\sim \frac{1}{3}(\mathcal{A}\lambda_1^k)^3 - \frac{5}{3}(\mathcal{A}\lambda_1^k)(\mathcal{B}\lambda_2^k)^2 + \dots, \\ \beta_k^{(2)} &\sim \sqrt{2}(\mathcal{A}\lambda_1^k)(\mathcal{B}\lambda_2^k) + \dots, \\ \beta_k^{(3)} &\sim \frac{4}{3}(\mathcal{A}\lambda_1^k)^2(\mathcal{B}\lambda_2^k) - \frac{2}{3}(\mathcal{B}\lambda_2^k)^3 + \dots.\end{aligned}\quad (\text{A16})$$

Inserting Eq. (A15) into the first line of Eq. (A6) yields

$$\begin{aligned}[X_k]_{11} = [X_k]_{22} &\sim -\zeta^{-1} \frac{\mathcal{A} + \mathcal{B}}{\sqrt{2}\lambda_{1,2}^k(\mathcal{A}^2 + \mathcal{B}^2)} + \zeta^0 \frac{1}{2} \\ &\quad - \zeta^1 \frac{\lambda_{1,2}^k(\mathcal{A} + \mathcal{B})}{6\sqrt{2}} + \dots, \\ [X_k]_{12} = -[X_k]_{21} &\sim \zeta^{-1} \frac{\mathcal{A} - \mathcal{B}}{\sqrt{2}\lambda_{1,2}^k(\mathcal{A}^2 + \mathcal{B}^2)} - \zeta^0 \frac{1}{2} \\ &\quad + \zeta^1 \frac{\lambda_{1,2}^k(\mathcal{A} - \mathcal{B})}{6\sqrt{2}} + \dots,\end{aligned}\quad (\text{A17})$$

where we have kept only terms to leading order in large  $\lambda_{1,2}^k$  for each order of  $\zeta$ . With the (global) exact solution in Eq. (A8), we

can easily identify  $\mathcal{A} = \mathcal{B} = \frac{1}{\sqrt{2}}$ , however a (local) asymptotic analysis does not provide such information. Thus, we would not realize the accidental cancellation of the  $\zeta^{\pm 1}$  terms in the off-diagonal elements of  $X_k$  in Eq. (A17). As those terms are appearing only as divergent as the ones on the diagonal, it will not affect the conclusions.

In summary, the RG would tell us that each component of  $X_k$  has the form

$$[X_k]_{ij} \sim \zeta^{-1} O(\lambda_{1,2}^{-k}) + \zeta^0 O(1) + \zeta^1 O(\lambda_{1,2}^k) + \dots.\quad (\text{A18})$$

Thus, by comparing the  $\zeta^{-1}$  term between Eq. (A18) and the expected form of the amplitude in Eq. (A14), we determine  $h(N) \sim \lambda_{1,2}^k = N$ . This allows us to conclude that  $\log_2 \lambda_1 = d_f$ , based on the fact that this relation has been observed on all networks studied thus far. This relation may seem obvious from  $\lambda_1^k = 2^k$  but could well be a mere coincidence. (For example, it would be wrong to conclude generally that  $\log_2 \lambda_2$  provides  $d_f$ .) Furthermore, comparing the  $\zeta^1$  terms provides that  $\lambda_{1,2}^k \sim 1/(N\theta_k^2)$ , i.e., that the temporal cutoff scales as  $\theta_k \sim \lambda_{1,2}^{-k} \sim 1/N$ , which implies by Eq. (1) that  $d_w^Q = \log_2 \lambda_{1,2} = 1$ . Note, though, that our main conclusion here is that by comparing order  $\zeta^0$  terms we *must* assume  $h(N) \sim N$  for a consistent interpretation, i.e.,  $O(N)$  such poles contribute to this result to make Eq. (A18) consistent with the corresponding expansion of Laplace poles in Eq. (A14). Luckily, we do not need to know anything *about* those poles.

- 
- [1] Y. Aharonov, L. Davidovich, and N. Zagury, *Phys. Rev. A* **48**, 1687 (1993).
- [2] D. A. Meyer, *J. Stat. Phys.* **85**, 551 (1996).
- [3] D. Aharonov, A. Ambainis, J. Kempe, and U. Vazirani, in *Proceedings of the 33rd Annual ACM Symposium on Theory of Computing (STOC 2001)* (ACM, New York, 2001), pp. 50–59.
- [4] J. Kempe, *Contemp. Phys.* **44**, 307 (2003).
- [5] A. Blumen and O. Mülken, *Phys. Rep.* **502**, 37 (2011).
- [6] R. Portugal, *Quantum Walks and Search Algorithms* (Springer, Berlin, 2013).
- [7] E. Venegas-Andraca, *Quant. Info. Proc.* **11**, 1015 (2012).
- [8] L. K. Grover, *Phys. Rev. Lett.* **79**, 325 (1997).
- [9] G. S. Engel, T. R. Calhoun, E. L. Read, T.-K. Ahn, T. Mancal, Y.-C. Cheng, R. E. Blankenship, and G. R. Fleming, *Nature (London)* **446**, 782 (2007).
- [10] H. B. Perets, Y. Lahini, F. Pozzi, M. Sorel, R. Morandotti, and Y. Silberberg, *Phys. Rev. Lett.* **100**, 170506 (2008).
- [11] A. M. Childs, *Phys. Rev. Lett.* **102**, 180501 (2009).
- [12] A. Schreiber, K. N. Cassemiro, V. Potoček, A. Gábris, I. Jex, and C. Silberhorn, *Phys. Rev. Lett.* **106**, 180403 (2011).
- [13] C. Weitenberg, M. Endres, J. F. Sherson, M. Cheneau, P. Schauss, T. Fukuhara, I. Bloch, and S. Kuhr, *Nature (London)* **471**, 319 (2011).
- [14] L. Sansoni, F. Sciarrino, G. Vallone, P. Mataloni, A. Crespi, R. Ramponi, and R. Osellame, *Phys. Rev. Lett.* **108**, 010502 (2012).
- [15] A. Schreiber, A. Gábris, P. P. Rohde, K. Laiho, M. Štefaňák, V. Potoček, C. Hamilton, I. Jex, and C. Silberhorn, *Science* **336**, 55 (2012).
- [16] A. Crespi, R. Osellame, R. Ramponi, V. Giovannetti, R. Fazio, L. Sansoni, F. D. Nicola, F. Sciarrino, and P. Mataloni, *Nat. Photon.* **7**, 322 (2013).
- [17] K. Manouchehri and J. Wang, *Physical Implementation of Quantum Walks* (Springer, Berlin, 2014).
- [18] V. V. Ramasesh, E. Flurin, M. Rudner, I. Siddiqi, and N. Y. Yao, *Phys. Rev. Lett.* **118**, 130501 (2017).
- [19] C. W. Duncan, P. Öhberg, and M. Valiente, *Phys. Rev. B* **95**, 125104 (2017).
- [20] H. Friedman, D. A. Kessler, and E. Barkai, *Phys. Rev. E* **95**, 032141 (2017).
- [21] *Random Walks and their Applications in the Physical and Biological Sciences*, edited by M. F. Shlesinger and B. J. West (American Institute of Physics, New York, 1984).
- [22] G. H. Weiss, *Aspects and Applications of the Random Walk* (North-Holland, Amsterdam, 1994).
- [23] B. D. Hughes, *Random Walks and Random Environments* (Oxford University Press, Oxford, 1996).
- [24] R. Metzler and J. Klafter, *J. Phys. A* **37**, R161 (2004).
- [25] S. Havlin and D. Ben-Avraham, *Adv. Phys.* **36**, 695 (1987).
- [26] N. Konno, *Quant. Info. Proc.* **1**, 345 (2002).
- [27] G. Grimmett, S. Janson, and P. F. Scudo, *Phys. Rev. E* **69**, 026119 (2004).
- [28] P. L. Krapivsky, J. M. Luck, and K. Mallick, *J. Phys. A* **48**, 475301 (2015).
- [29] A. Ambainis, J. Kempe, and A. Rivosh, in *Proceedings of the Sixteenth Annual ACM-SIAM Symposium on Discrete Algorithms, SODA '05* (SIAM, Philadelphia, 2005), pp. 1099–1108.



- [30] N. Inui, N. Konno, and E. Segawa, *Phys. Rev. E* **72**, 056112 (2005).
- [31] S. Falkner and S. Boettcher, *Phys. Rev. A* **90**, 012307 (2014).
- [32] S. Boettcher, S. Falkner, and R. Portugal, *Phys. Rev. A* **90**, 032324 (2014).
- [33] A. Maritan and A. Stella, *J. Phys. A* **19**, L269 (1986).
- [34] H. A. Ceccatto, W. P. Keirstead, and B. A. Huberman, *Phys. Rev. A* **36**, 5509 (1987).
- [35] V. Kendon, *Math. Struct. Comput. Sci.* **17**, 1169 (2007).
- [36] A. Romanelli, R. Siri, G. Abal, A. Auyuanet, and R. Donangelo, *Physica A (Amsterdam)* **347**, 137 (2004).
- [37] S. Redner, *A Guide to First-Passage Processes* (Cambridge University Press, Cambridge, England, 2001).
- [38] S. Boettcher, S. Falkner, and R. Portugal, *J. Phys.: Conf. Ser.* **473**, 012018 (2013).
- [39] S. Boettcher, S. Falkner, and R. Portugal, *Phys. Rev. A* **91**, 052330 (2015).
- [40] M. Szegedy, in *Proceedings of the 45th IEEE Symposium on the Foundations of Computer Science* (IEEE, New York, 2004), pp. 32–41.
- [41] F. Magniez, A. Nayak, P. C. Richter, and M. Santha, in *Proceedings of the Twentieth Annual ACM-SIAM Symposium on Discrete Algorithms, SODA '09* (SIAM, Philadelphia, 2009), pp. 86–95.
- [42] S. Boettcher, S. Li, and R. Portugal, *J. Phys. A* **50**, 125302 (2017).
- [43] M. Plischke and B. Bergersen, *Equilibrium Statistical Physics*, 2nd ed. (World Scientific, Singapore, 1994).
- [44] S. Boettcher, S. Li, T. D. Fernandes, and R. Portugal, [arXiv:1708.05339](https://arxiv.org/abs/1708.05339).
- [45] S. Boettcher and J. L. Pughe-Sanford, [arXiv:1709.06414](https://arxiv.org/abs/1709.06414).
- [46] A. N. Berker and S. Ostlund, *J. Phys. C* **12**, 4961 (1979).